CHAPTER II
# BACKGROUND AND LITERATURE SURVEY

2.1 Background SnO₂ Gas Sensors

Gas sensor devices can be divided into three groups depending on the technology applied in their development solid state, spectroscopic and optic. Spectroscopic systems are based on a direct analysis of the molecular mass or vibration spectrum of a target gas. These sensors can measure quantitatively the composition of the different gases with a good precision. Mass chromatograph and mass spectrograph are the most important gas sensor spectroscopic systems. Optical sensors measure absorption spectra after the target gas has been stimulated by light. This kind of sensors requires a complex system: a monochromatic excitation source and an optical sensor for the analysis of the absorbed spectra. While spectroscopic and optical systems are very expensive for domestic use and sometimes difficult to implement in reduced spaces as car engines, the so-called solid state sensors present great advantages due to their fast sensing response, simple implementation and low prices. These solid state gas sensors are based on the change of the physical and/or chemical properties of their sensing materials when exposed to different gas atmospheres.

The semiconductor gas sensor (SGS) is the solid-state gas sensors: present the property of changing the conductivity of the sensing material in presence of a determinate gas. A simple SGS is composed of a substrate (where sensor material will be supported), electrodes (to measure the conductivity change) and heaters (to reach the optimum sensing temperatures). There are three parameters related to an improvement of an accuracy of device: its sensitivity, selectivity and stability. The sensitivity is the device characteristic of perception a variation in physical and/or chemical properties of the sensing material under gas exposure. The selectivity is related to the discrimination capacity of a SGS device in presence of a mixture of gases. The stability is a characteristic that takes into account the repeatability of device measurement after a long use. (*http://nun97.el.ub.es/~arbiol/discdos /nanopart/tesi/tesi1.pdf*)

Semiconductor sensors detect gases via variations in their resistances or conductance. It is well known that sensors consisting of fine particles of metal oxides tend to exhibit high sensitivity. Thus one of the most important factors affecting sensing properties is the actual gain or crystallite size of the sensor materials in the conjunction with the space-charge depth (L). Pure SnO_2 sensors have been shown to exhibit drastic changes in resistance as a function of grain size.
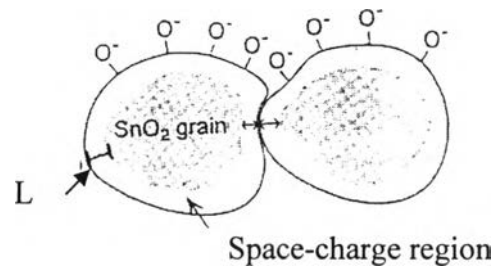
Figure 2.1 Space-charge depth (L) (Shimizu and Egashira 1999).

It is generally accepted that the conductivity of such gas sensing layers for thick and porous films is controlled by the Schottky barrier that appears at the junctions of adjoining grains. The Schottky barrier height and the conductivity of the material are modulated by the surface coverage of the material with chemisorbed charged species of oxygen, particularly with O^- and O^{2-} ions. For an n-type semiconductor (the tin dioxide is an n-type semiconductor), a negative charge density, σ accumulated on the surface increases the Schottky barrier height (V_s) according to the relation:

$$V_s = \frac{\sigma^2}{2 \cdot \varepsilon \cdot N_D \cdot e} \qquad (2.1)$$

Where N_D is the bulk donor concentration; e and ε are the elementary charge and the dielectric constant of the semiconductor, respectively.

The gas-sensing process in such gas sensors has two steps:

- Chemisorption of oxygen as charged O^{2-} or O^- species creating on the rise of the Schottky barrier heights at the junctions between grains and therefore a decrease of the conductivity.

- Decrease of the surface coverage with chemisorbed oxygen by the reducing gas and, as a consequence, increasing of the conductivity.

The SnO_2 is an n-type semiconductor. The donor states are usually associated with the oxygen bulk vacancies. The first step of the sensing mechanism is the "sensitising" chemisorption of oxygen. The oxygen molecules are chemically adsorbed on various sites of the tin dioxide surface as O_{ads},

$$O_2 \longleftrightarrow 2O_{ads} \tag{2.2}$$

In the SnO_2 lattice, the oxygen appears as O^{2-}; the oxygen adsorption creates surface acceptor states O/O^-_{ads} and O^-/O^{2-}_{ads} on which conduction electrons will be trapped. These electronic states are placed on the band diagram below the Fermi level as shown (Figure 2.2)

$$O_{ads} + e^- \longleftrightarrow O^-_{ads} \tag{2.3}$$

$$O^-_{ads} + e^- \longleftrightarrow O^{2-}$$
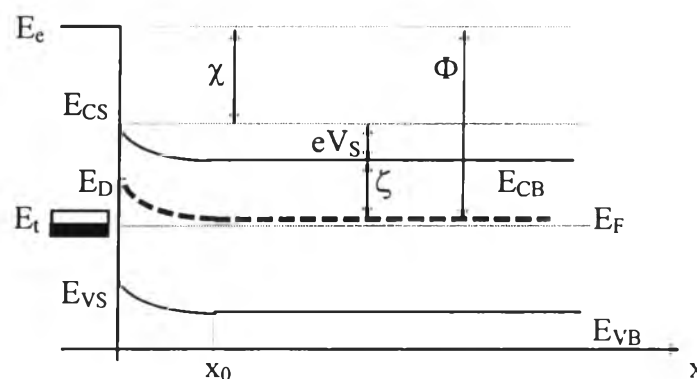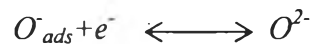
Figure 2.2 Surface Schottky-barrier profile with pinned Fermi level.

Where:

E_{VB} = Energy of valence band

E_F = Energy of Fermi level

E_{CB} = Energy of conduction band

Φ = The m-site grand-partition function

ζ = The 1-site grand-partition function

χ = The grand-canonical potential

The effect of the reducing gas is to reduce the chemisorbed oxygen. As a consequence, the surface net charge is lowered and the trapped electrons are released back to the conduction band. The reaction corresponding to this process is:

$$RO^{2-} \longleftrightarrow RO+2e^- \tag{2.4}$$
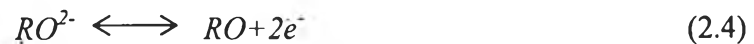
By replacing this equation into the equation (2.1), one obtains, for the surface Schottky-barrier height:

$$V_S = \frac{V_0}{\left(1+\rho\dfrac{p}{\Pi}\right)^2} \tag{2.5}$$

Where p is the partial pressure of the reducing gas, ρ and Π are the numeric parameter that used in the calculation of adsorption model. V_0 is the barrier height in the absence of the reducing gas:

$$V_0 = \frac{2 \cdot e \cdot N_s^2}{\varepsilon \cdot N_D} \tag{2.6}$$

Further on we will use the following notations:

- N_S -Density of surface adsorption sites for oxygen.
- n - Bulk concentration of conduction electrons.
- N_D - volume concentration of donors (oxygen vacancies)

The conductivity of the sensor will be given by:

$$G=env \tag{2.7}$$

Where v is the bulk mobility and n is the concentration of the electrons. Not all the electrons have a high enough energy to overpass the Schottky barrier, though. According to the Maxwell-Boltzmann statistics, the conductance may be written:

$$G = enve^{-\frac{eV_S}{kT}} \qquad (2.8)$$

By analogy of equation (2.5) and new definition for and by defining, conductivity in clean air (G_0),

$$G_0 = enve^{-\frac{eV_0}{kT}} \qquad (2.9)$$

One obtains the normalized sensitivity of the sensor (G/G_0 ratio),

$$\frac{G}{G_0} = \exp\left(\frac{eV_0}{kT}\left(1 - \frac{1}{1+\rho\frac{p}{\Pi}}\right)\right) \qquad (2.10)$$

In the absence of the reducing gas (p=0), equation (2.10) implies a value for the sensitivity equal to 1. At high pressures, when $\rho(p/\Pi) \gg 1$, the sensitivity reaches a saturation value:

$$\left.\frac{G}{G_0}\right|_{sat} = e^{\frac{eV_0}{kT}} \qquad (2.11)$$

From equations (10) and (11), one can write the response function as:

$$\frac{G}{G_0} = \left(\left.\frac{G}{G_0}\right|_{sat}\right)^{\left(1-\frac{1}{1-\beta c}\right)} \qquad (2.12)$$

Where c is the gas concentration in ppm, $(G/G_0)_{sat}$ and β are parameters which will be determined by fitting the equation with the experimental data.
*(www.physics.mcgill.ca/~fluerasu/research/mech.doc)*

2.2 Microemulsion Method

Microemulsion method was invented as an effective process of preparing nanoparticles in the 1980s. Spherical powder with uniform dimensional distribution and good dispersibility can be obtained by such method via adjusting the size of reactors and other reaction conditions. Microemulsions are colloidal 'nano-dispersions' of water in oil (or oil in water) stabilized by a surfactant film. These thermodynamically stable dispersions can be considered as truly nanoreactors that can be used to carry out chemical reactions and, in particular, to synthesize nanomaterials. The main idea behind this technique is that by appropriate control of the parameters one can use these nanoreactors to produce tailor-made products down to a nanoscale level with new and special properties.

The shape and size of the dispersed nanodroplets is mainly governed by the curvature free energy and is determined by the elastic constant and the curvatures of the surfactant film. The elasticity of the film depends not only on the surfactant type and the thermodynamic conditions, but also on the presence of additives, like alcohols, electrolytes, block copolymers and polyelectrolyte. In the past, mainly spherical (and in some cases elongated) nanodroplets have been used to prepare nanoparticles of different kind of materials such as Cu, Zr, Ni and Pd and it was assumed that the size and shape of these nanodroplets could 'template' the synthesis of nanomaterials. However, one has to take into account the dynamic nature of the microemulsions. Due to the Brownian motion these droplets collide forming a fused dimer (or an encounter pair) and interchange reactants with a rate constant k_{ex}. The above-described parameters, which determine the elasticity of the surfactant film, influence also the reactant interchange among the nanodroplets. The interdroplet exchange of the particles growing inside the droplets is inhibited by the inversion of the film curvature in the fused dimer, which, in turns, depends on the film flexibility (Figure 2.3). All of this has to be taken into account to understand the particle size control in microemulsions. Because a lot of parameters with different influences enter into consideration the film flexibility through a parameter, f proportional to $k^{-3/2}$ being k the curvature elastic modulus; the interdroplet exchange rate constant k_{ex}; concentration of reactants c; reactant excess ratio x; droplet size R (which is

controlled by the ratio $w=$ ([H$_2$O] / [surfactant]); volume fraction Φ; and critical nucleus n^*.
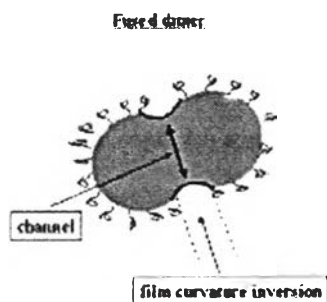
Figure 2.3 Schematic representation of a fused dimer after a two droplets collision showing the channel opened in between. The inversion of the film curvature in this channel is shown. (Lopes-Quintela, M.A., 2003).

Two more aspects were considered in the simulation, namely, the possibility of autocatalysis of the reaction by the already formed sub-nanoparticles (clusters) and the possibility of ripening. Until now only a restricted parameter space could be explored assuming that mixing two identical microemulsions carrying the reactants performs reactions. It turns out that many of the previous ideas putted forward to explain the experimental results, based in the well-known bulk nucleation and growth models, and are not longer valid for the particle formation in these dynamic compartmentalized media. The reactant excess hardly influences the nucleation process but, on the contrary, it has a great influence on the growth mechanisms. In these compartmentalized media growth by ripening is limited by the channel size opened in the fused dimer whereas growth by autocatalysis is only limited by the reactant concentration. Many conclusions of the synthesizing have been published such as:

- Control of particle size by reactant concentration. The increase of particle size (and polydispersity) by increasing the concentration is predicted.
- Decrease of particle size by increasing the excess of one of the reactants until a plateau is reached at high excesses.

- Increase of particle size by increasing the surfactant film flexibility. The increase in flexibility can be achieved by increasing the amount of co-surfactant (alcohols), approaching to the microemulsion instability phase boundaries, changing the droplet size, changing the chain length of the oil or co-surfactant, etc.

- Increase of particle size by increasing the droplet size. In principle, a linear relationship should be expected, but one has to consider that, in many cases, because of the associated increase of the flexibility with droplet size these two effects are superimposed and a much larger increase of the particle size is observed. This effect should be less important working with more rigid surfactant films (Lopes-Quintela, M.A., 2003).

The surfactants are molecules with distinct hydrophobic and hydrophilic regions. Depending on their chemical structures, the surfactants can be non-ionic, cationic, anionic or zwitterionic. An example of a non-ionic surfactant is alkylphenolalkoxylates, such as Triton X-100.Examples of cationic surfactants includes alkylammonium salts, such as hexadecyltrimethylammonium bromide. Anionic surfactants can include metal salts of organosulfonates and organosulfosuccinates, such as sodium dodecylsulfate (SDS) and sodium bis (2-ethylhexyl)sulfosuccinate (NaAOT), respectively. Examples of zwitterionic surfactants include 3-(dimethyldodecyl-ammonium) propane sulfonate and cethyltrimethylammonium p-toluene sulfonate. The hydrophobic part of the surfactant can be of various lengths, e.g., 8 to 20 carbon atoms, contain multiple bonds, or consist of two or more hydrocarbon chains. Preferred surfactants useful for forming the reverse micelles and microemulsions of the present invention include alcohol ethoxylates, alkylphenolethoxylates, silicone surfactants and alkylpolyglycosides. The different of surfactant form the different size of droplets in the microemulsion system. Such as when the solubilization of water, or the polar phase, into the low or non-polar phase by a nonionic surfactant is poor, it need to enhance the properties of surfactant and reduce the size of droplet by the addition of a co-surfactant, such as an alcohol having from 5 to 10 carbon atoms. Preferred co-surfactants are pentanol, hexanol, and octanol, individually or in combination. Preferably, the weight ratio of co-surfactant to surfactant is about 1:5 to2:3.

Therefore, the different of the surfactant structure is the one effect to the size of reverse micelle that related to the size of particles. Typically, the surfactant and co-surfactant, in a specific ratio, are mixed first to form a blend. The blend is then mixed with the low or non-polar phase to form a homogenous blend solution. Preferable blend content in the solution is about 5 to about 30 vol. %. The low or non-polar phase can be cyclohexane, hexane, hexadecane, isooctane, alkylated benzenes, polyaromatic hydrocarbons, linear and branched paraffins, napththenes, petroleum distillates, mineral oil, and linear or cyclic siloxanes. Suitable polar solvents are water, monohydric, dihydric, and trihydric alcohols and organic nitrites, which have dipole moments greater than one Debye and dielectric constants greater than 6 at 20-25 °C. Water is the preferred polar solvent. Preferably, the polar phase to surfactant molar ratio, w, is less than about 30, more preferably from about 4 to 25, and most preferably from about 6 to about 12 (Lewis et al. 2004).

2.3 Literature Survey

Many researchers investigate many methods to improve the sensitivity of gas sensors especially tin oxide gas sensor. The effect of ppm level H_2 on the direct current resistance of SnO_2 particle size variation is studied and reported by Ansari *et al.* (1997). Stannic oxide (SnO_2) was used as the basic material for the sensor. SnO_2 nanoparticles were synthesized using the sol-gel method with the change in calcinations temperature. The thick films were prepared using standard screen printing technology. The paste, thus formulated was printed on alumina substrate (12 mm x 25 mm). The measured particle sizes were used only to detect the changes occurring with increasing temperature. The SnO_2 crystallite size, D, is varied in the range of 20-50 nm and sensitivity for H_2 is found to increase steeply as D decreases.

In 1998, Li and Kawi investigated the effect of the surface area of SnO_2 to the sensitivity tin oxide gas sensors. The high surface area SnO_2 materials were systematically synthesized by a surfactant incorporating method. After calcinations at 723 K, a high BET surface area of $156.8 m^2$ /g was obtained. The sensing properties of the high surface area SnO_2 material were studied using H_2 as the probing gas. The results are the high surface–area SnO_2 sensors could be a highly–

sensitive and thermally stable gas sensor to detect very low concentration of reducing gases even at high temperature. It is found that a linear relationship exists between sensor surface area and it's sensitive to H_2

Martinelli *et al.* (1999) studied the effective of gas sensors in environmental monitoring applications, outdoor field tests were performed using the prepared thick-film prototype sensors and reviewed their work on the use of semiconducting oxide powders for the fabrication of thick films by screen-printing technology. The sensor array was placed beside a traffic light in the city of Ferrara, Italy, co-located with a conventional environmental monitoring station controlled by the Ferrara section of ARPA (the Regional Agency for Pollution Prevention). The sensors responses were compared with the concentrations of the major pollutants (CO, CO_2, NO, NO_2, ozone, etc.) in the atmosphere, as measured using methods approved by international standards. These results obviously showed only qualitative and not quantitative polluting-gas–monitoring capabilities, nevertheless, an attempt was made to find quantitative correlation between the concentrations measured by convention analytical equipment and the sensor outputs, using calibration curves. The calibration curves were used to evaluate quantitatively the CO and NO concentrations from the electrical response of SnO_2 and $LaFeO_3$ sensors, and they showed good agreement with the values measured with standard analytical equipment, although there were large errors involved in this procedure (which neglected the influence of interference gases on sensor response). However, phenomena such as inversion temperatures also make valid evaluation difficult, due to NO_2 and O_3 interference. This problem might be overcome by increasing the number of sensors in the array, particularly with materials able to selectively detect these gases.

In 2001, Fau *et al.* studied the tin oxide nanoparticles sensitive layer on the silicon platform for domestic gas application. The micromachined silicon platforms have been specially created to be coated with a drop of tin oxide sensitive layer. Design of the silicon substrate includes a thin dielectric membrane for mechanical and thermal insulation purpose. A passivity layer covers the silicon front side structures except bonding pads and sensitive layer contacts and allows an easy drop deposition (no short circuit risk with heater electrode). The deposition material is a suspension of tin dioxide nanoparticles mixed in a solvent. A novel drop deposition

show high sensitivity and reliability level. They have described a new promising way to realize micromachined silicon gas sensors based on thick films of tin oxide nanoparticles. These sensors show high sensitivity to carbon monoxide and methane. They also show sensors in very stable baseline resistance and gas sensitivity over time. These particular features and attributed to the nature of the sensitive layer, which consist of spherical and chemically pure particles of tin oxide correlated with a tight distribution in size and shape. In addition, their process allows the deposition of the sensitive layer on each device at the end of process. This ensures chemical purity of the tin oxide, which is essential for the stability and the reproducibility of the sensor.

However, many scientists try to improve the ability of this sensor such as Meixner and Lampe (1996) investigated a new gas sensor, which will be used to replace tin oxide sensors in the future, the heterometallates gas sensors. The heterometallates metals are complex combinations with the general compositionally $A_nXM_{12}O_{40}$, whereby A is a monovalent cation, n=3 or 4, X is P, Si or As and M is W or Mo. These oxides have been known for many years as selective oxidation catalysts. Although these combinations have some potential for use as gas-sensitive materials, their gas-sensitive properties have only been investigated thoroughly. This also holds true for the description of these oxides as thin films. In comparison to the sensors based on SnO_2 their properties are improved in several items. The main improvements are the lower influence of humidity, the long-term stability, the ability to start measurement immediately after switch on and reduced unit spread but can use with only few gases.

One year later Schweizer-Berberich *et al.* studied the effect of doping on the response of nanoparticles tin dioxide gas sensors to carbonmonoxide. Compared with the "classical" tin dioxide sensors, this new class of device offers an increased sensitivity and selectivity. SnO_2 sensors were prepared by precipitating $Sn(OH)_4$ from an aqueous solution of $SnCl_4$ or by evaporating SnO_2 in the high vacuum. The effect of Pt and Pd doping upon the response to CO is studied. Parameters, which they focused on, are sensor signal dependent on the operating temperature and dependent on the gas concentration. The thicknesses of the ceramic materials were between 0.1 and 1 mm. The dependence of the conductance G on the CO

concentration (in the 100-500 PPM range) may formally be described by for all sensor types and all heating voltages.

$$G = \text{const. x } (Pco)^n$$

The value of the parameter n is related to the chemical surface reaction between CO and chemisorbed oxygen. The results show that both the sensitivities and parameter n of a power law of thin and thick film sensors are varied. Thick film sensors (especially the doped ones) show higher sensitivities to detect CO due to the more porous structure of the material and the parameter n (of a power law) reaches higher values. The factor n can also be varied due to another reaction mechanism because of changes in the operating temperature. The Pt and Pd doping resulted in a shift of the maximum of sensitivity and factor n to lower operating temperatures. The sensitivity itself is enhanced (dramatically for ceramic sensors).

Liu *et al.* investigated the doping metals on the tin oxide gas sensors again in year 2000. The structure of SnO_2 thin films doped with Pd, Sb, Pt and In, especially the effects of dopants on the electronic structure of SnO_2 were studied by XPS and TEM. The focus was mainly put on the influence of dopants and H_2 adsorption on the electronic structure of SnO_2, because the conduction electrons of SnO_2 film play a major role in gas sensing and will change with exposing to the gas to be detected. The results are the kind of dopant Sb, Pd, Pt or in hardly changed the grain size of SnO_2 thin film within low doping amount, but they did change the Fermi level of SnO_2 but also influenced the distribution of electron state density (DESD) of Sn4d valence band. They also studied the electronic structure change of the doped SnO_2 after H_2 adsorption. The H_2 adsorption influenced not only the chemical states of Sb and Pd in the films but also the electronic structures of SnO_2, including the Fermi level and the DESD of Sn4d valence band. At the same time Mukhopadhyay *et al.* reported, for the first time, the details of structural and deposition characteristic of the tin oxide thin film as a function of experimental parameters such as the number of dipping, bath temperature and bath concentration. In addition, the electrical properties were studied for both as deposited and palladium sensitized films as a function of temperature (300-500 K) in a closed quartz tube

furnace. Further, the gas sensitivity of the palladium sensitized tin dioxide thin film sensors was evaluated in air inside the same closed quartz tube furnace as a function of the operating temperature (150-300°C) for a fixed concentration (3 vol%) of hydrogen gas with nitrogen gas as the carrier gas. The sensor response could be recorded at an operating temperature of as low as 150°C. Maximum sensitivity of 90% was found to occur at a low temperature of only 200°C. Above this cut temperature, sensitivity of the thin film sensors was found to suffer only moderate degradation. The tin dioxide thin films were deposited on pre-cleaned substrates. Commercially available microscope glass slides of 2.1-mm thickness were used as substrates.

From many literatures above, they describe the development and application of tin oxide gas sensors. However, an important point, it has also told that an increasing the surface area of tin oxide increase the sensitivity of gas sensor. The literatures below will show the improvement of the microemulsion methods that use to synthesize the metal nanoparticles, which is also increasing the surface area of particles. In 1996, Qi *et al.* studied the preparation of $BaSO_4$ nanoparticles in nonionic w/o microemulsions. Spherical and cubic $BaSO_4$ nanoparticles with barite structure were synthesized (below 20 nm) in Triton X-100/n-hexanol/cyclohexane /water water-in-oil microemulsion by mixing two separated prepared microemulsion containing $(NH_4)_2SO_4$ and $Ba(OAc)_2$. The effect of water content and presence of $(NH_4)_2SO_4$ on the size of the microemulsion droplets were investigated by dynamic light scattering. Particle characterization was accomplished by transmission electron microscopy and the effects of water content, holding time; surfactant content and reactant concentration on the particle characteristics were studied. Due, to the cage-like nature of the microemulsion droplets, the size of the microemulsion droplets has a controlling effect upon the size of the particles prepared. The results indicate that the size of the microemulsion droplets increases with the water content in microemulsions. The water content greatly affects the shape of the $BaSO_4$ particles prepared. The particle shape was found to convert from spherical to cubic as the water content in the microemulsion increases. It has been shown that monodisperse cubic $BaCO_4$ nanoparticles can be produced inside spherical microemulsion droplets under suitable conditions. Spherical particles are obtained when the water content is

smaller, while cubic particles can be prepared from microemulsions with higher water content. The size of the microemulsion droplets has a controlling effect upon the size of the particles prepared from the microemulsions, i.e. the size of the particles increases with the size of the microemulsion droplets. The particle size polydispersity increases as the water-to-surfactant molar ratio (w) is increased.

One-year later Qi *et al.* studied the synthesis of nanoparticles by the microemulsion method again but in this year they investigated the synthesis of copper nanoparticles in nonionic water-in-oil microemulsions. Metallic copper nanoparticles have been prepared by reduction of the simple copper ion salt $CuCl_2$ in TX-100/n-hexanol/cyclohexane/water w/o microemulsion using $NaBH_4$ as reduction agent. The prepared copper particles were characterized by transmission electron microscopy and absorption spectroscopy. The result from this experimental has been shown that well-dispersed metallic copper particles are formed in w/o microemulsion, whereas only associated copper oxides particles are obtained when the reaction is performed in the aqueous solution. This result could be explained in terms of the high local copper concentration in water pools of the microemulsions. The absorption spectrum of the copper particles synthesized in microemulsion shows the lack of the plasmon band characteristic of the Cu surface, which could result from the formation of the $CuCl_2$ monolayer on the copper particles.

The nanoparticles of tin oxide (SnO_2) have been prepared from water-in-oil microemulsions consisting of water, AOT (surfactant), and n-heptane (oil) (Song and Kim, 1999). The aqueous phase in the water in oil microemulsion was a solution of 0.1 M $SnCl_4$ while the molar ratio of water to AOT in microemulsions was 20. Precursor hydroxides were precipitated in the aqueous cores of water-in-oil microemulsions and then calcined at 600°C for 2 h to form tin oxide powder. The formation of phase pure tin oxide was confirmed by means of X-ray diffraction analysis (XRD). The tin oxide powder was found to be less than 40 nm in particle diameter and to have a higher specific surface area, about 73 m^2/g, when compared with tin oxide powder prepared though the conventional precipitation method (19m^2/g). From this result, it was found that the microemulsion method as presented in this study is effective for synthesizing tin oxide powder with a higher surface area which is expected to increase the sensitivity of chemical gas sensors. In the same

year, Li and Wang (1999) studied the nanometer-sized titania particles that have been prepared by chemical reactions between $TiCl_4$ solution and ammonia in reversed microemulsion systems. Cyclohexane and a mixture of poly (oxyethylene)$_5$ nonyle phenol ether and poly (oxyethylene)$_9$ nonyle phenol ether with weight ratio 1:1 are used as oil phase and nonionic surfactant (NP5-NP9), respectively. The product is characterized by transmission electron microscope, Raman spectroscopy, differential thermal and thermogravimetric analyses. Size distribution of particles determined from electron micrographs fits well with a lognormal function whose values for median and width are 5.4 nm and 1.4 nm. The crude product is amorphous and transforms into anatase heated at temperature from 200 to $750^{\circ}C$, into rutile at temperatures higher than $750^{\circ}C$.

One year later, Alany *et al.* (2000) studied the effect of alcohols and diols on the phase behavior of quaternary systems. The aim of the study was to investigate the effect of different co-surfactants on the phase behavior of the pseudoternary system water: ethyl oleate: nonionic surfactant blend (sorbitan monolaurate/polyoxyethylene 20 sorbitan mono-oleate). Four aliphatic alcohols (1-propanol, 1-butanol, 1-hexanol and 1-octanol) and four 1,2-alkanediols (1,2-propanediol, 1,2-pentanediol, 1,2-hexanediol and 1,2-octanediol) were used. The co-surfactant-free system forms two different colloidal structures, a water-in-oil microemulsion (w/o ME) and lamellar liquid crystals (LC) and two coarse dispersions, water-in-oil (w/o ME) and oil-in-water emulsions (o/w EM). Microemulsion region area (%ME), liquid crystalline region area (%LC), amount of amphiphile (%AMPH) blend required to produce a balanced microemulsion and amount of water solubilised (%W) were used as assessment criteria to evaluate the co-surfactants. Seven calculated physico-chemical descriptors were used to represent the different co-surfactants. 1-butanol, 1, 2-hexanediol and 1, 2-octanediol produced balanced MEs capable of solubilising a high percentage of both oil and water. A similarity was observed between the descriptors attributed to 1-butanol and 1, 2-hexanediol. The requirements of a co-surfactant molecule to produce a balanced microemulsion were: HLB value 7.0-8.0, a carbon backbone of 4-6 atoms, percentage carbon of 60-65%, percentage oxygen of 20-30%, log P value of 0.2-0.9 and log 1/S (S: aqueous solubility) close to zero.

The studies of the nanoparticles tin oxide were investigated again by Song and Kim (2000). The tin oxides have been synthesized from water-in-oil microemulsions consisting of water, AOT (surfactant), and n-heptane (oil) similar to their previous (Song and Kim, 1999) but the molar ratio of water to AOT in microemulsions was 15. This work shows that it is possible to prepare tin oxide powder with high surface area by the water-in-oil microemulsion method. When the precursor powders from the microemulsion method were calcined at 600 $^\circ$C for 2 h they exhibited a higher Brunauer-Emmet-Teller (BET) surface area of 86 m^2/g. On the other hand, the powders obtained from the conventional precipitation method showed a lower surface area of 19 m^2/g. And they have also seen in the pore size distributions of the powders prepared by the microemulsion and the precipitation method, respectively. The pore structure of the precipitation-derived powder was monomodal. There was a maximum for the pore diameter at 10.8 nm. On the other hand, the pore size distribution of the microemulsion-derived powder showed two maximum values at 3.7 and 4.7 nm. It was also shown that the powder from the microemulsion method has smaller pores than that from the precipitation method.

One year later, the effect of nonionic surfactant to the synthesis and characterization of silica-coated iron oxide nanoparticles in microemulsion were studied by Santra *et al.* (2001). Three different nonionic surfactants (Triton X-100, Igepal CO-520, and Brij-97) have been used for the preparation of microemulsions and their effects on the particle size, crystallinity, and the magnetic properties have been studied. The iron oxide nanoparticles are formed by the co-precipitation reaction of ferrous and ferric salts with inorganic bases. A strong base, NaOH, and a comparatively mild base, NH_4OH, have been used in each surfactant to observe whether the basicity has some influence on the crystallization process during particle formation. Transmission electron microscopy, X-ray electron diffraction, and superconducting quantum interference device magnetometry have been employed to study both uncoated and silica-coated iron oxide nanoparticles. All these particles show magnetic behavior close to that of superparamagnetic materials. By use this method, magnetic nanoparticles as small as 1-2 nm and of very uniform size (percentage standard deviation is less than 10%) have been synthesized. A uniform silica coating as thin as 1 nm encapsulating the bare nanoparticles is formed by the

base-catalyzed hydrolysis and the polymerization reaction of tetraethyl orthosilicate in microemulsion. All experimental results are also compared with those for particles synthesized in pure water.

Ultrafine titania particles were prepared from reacting $TiOCl_2$ with NH_4OH in the nanodroplets of water/Triton X-100/n-hexanol/cyclohexane microemulsions. The as-prepared particles were amorphous, transformed into the anatase phase at 460°C, and further into the rutile phase at 850°C. The crystallite size of the particles was in the range of 10-36 nm at temperatures between 500 and 900°C. Secondary particles were 40-50 nm in size at 500°C and increased markedly by a factor of 10 at 900°C due to a significant interagglomerate densification. With increasing calcinations temperature from 300 to 900°C, the specific surface area of the particles decreased rapidly from 317.5 to 8.4 m^2/g, while the average pore radius increased considerably from 2.9 to 31.8 nm as the result of shrinkage and densification of the agglomerates and destruction of the minute intercrystallite pores. The anatase phase formed at 500-700°C showed considerable photoavtivity for the degradation of phenol, whereas both the amorphous phase at 300°C and the rutile phase at 900°C were inactive for this reaction. (Kim and Hahn, 2001)

In 2002, Kuang *et al.* study the preparation of inorganic salts ($CaCO_3$, $BaCO_3$, and $CaSO_4$) nanowires in the Triton X-100/cyclohexane/water reverse micelles. The growth process of $CaCO_3$ nanowires was monitored by the transmission electron microscopy (TEM). TEM images reveal that the $CaCO_3$ nanowires were formed in the reverse micelles by the direction aggregation process. The nanowires of $CaCO_3$ were 5-30 nm in diameter and had a length more than 10 μm. $BaCO_3$ nanowires were also prepared in the TX-100 reverse micelle. It can be clearly seen that many wire were disordered pack with length up to several ten of micrometers. Higher magnification TEM image shows the wires with diameter in the range of 5-20 nm and irregularly arrayed. $CaSO_4$ nanowires were also prepared in the TX-100/cyclohexane/water reverse micelle. Some wires with diameter less than 30 nm and length more than 2 μm were obtained.

One year later, Guo *et al.* (2003) used the reverse microemulsions (RMs) to prepare ceramic inks for jet-printing formation. First of all, different RM systems were chosen and optimized in order to obtain high concentration ceramic inks. Triton

X-100/co-emulsifier/oil/water RM system was systematically investigated. Different kinds and different amounts of co-emulsifier and oil phase were selected and mixed to form RM after intensively stirring. RM region in the quasi-ternary phase diagram of the system was determined. It was shown that Triton X-100/n-hexanol/cyclohexane/water RM system exhibited an excellent behavior in enhancing water-dissolving amount. The best composition for the maximum water content was given. Zirconium oxychloride solution and ammonia solutions were then added to the above system respectively. After stirring intensively, two clear RMs were obtained. Then ZrO_2 ceramic inks were readily prepared by the reaction after mixing the two RMs uniformly. The physicochemical properties of ZrO_2 ceramic inks, such as viscosity, surface tension, conductivity, stability etc. were determined. The particle size and morphology of ZrO_2 nanoparticles in the RM were observed by TEM. The RM was prepared at $20^{\circ}C$, using Triton X-100 as emulsifier; n-butanol, n-pentanol, and n-hexanol as co-emulsifier respectively; cyclohexane, n-heptane, and n-octane as the oil phase and deionized water. Triton X-100 and co-emulsifier were combined in the ratio of 1:0, 4:1, 3:2 and 1:1 respectively, intensively stirred to as S+A phase (the surfactant combine with the co-surfactant phase). The oil phase was combined with the above liquid S+A in the ratio of 5:1, 4:1, 3:1, 2:1, 1:1, 1:2, 1:3, 1:4 and 1:5, and strongly stirred for 10 min for later use. Different amounts of deionized water were added to the above mixture. They were strongly stirred again for 30 min and settled for 2 days. Then the formation of reverse microemulsion was determined through visual observation, conductivity measurement and centrifugal separation, which revealed the phase transformation or phase separation of the ternary system. Finally, the quasi-ternary phase diagrams of the systems were given and the maximum water content for each system was determined. The results of the experiment show that

1. Triton X-100/n-hexanol/cyclohexane/water reverse microemulsion system was chosen and optimized from several other systems of reverse microemulsion to prepare ZrO_2 ceramic ink because it exhibited an excellent behavior in enhancing water – dissolving amount.

2. The best composition for the maximum water content of the above system was 19.1% Triton X-100/12.8% n-hexanol/23.7% cyclohexane / 44.4% water in mass determined by its quansi-ternary phase diagram.

3. Two clear reverse microemulsions were obtained by replacement of the water in the system with equivalent volume of zirconium oxychloride solution and ammonia solution, respectively.

4. ZrO_2 ceramic inks prepared by reaction after mixing the two reverse microemulsions uniformly demonstrated excellent stability, dispersivity and homogeneity

5. They were suitable for ink-jet printing forming by a drop on demand ink-jet printer through determinations of the physicochemical properties of the inks, such as viscosity, surface tension and transparency etc.

6. Their conductivity was not sufficiently high according to the requirements of the printer due to the continuous phase of oil.

7. The particle size in the reverse microemulsions was about 7-10 nm and very well dispersed by TEM observation.

8. It is still necessary to increase the solid load in the suspension further.

The formation of zinc sulfide nanorods and nanoparticles in ternary W/O microemulsions were studied. Appropriate three-component microemulsion system can be optimized and employed to obtain 1-D nanocrystals of ZnS. By adopting ternary microemulsion system, Triton X-100 or CTAB/cyclohexane/water, nanorods of ZnS can be synthesized under appropriate conditions, with lengths up to 6 μm and diameter 12-85 nm. Varying different variables shows that wo = 11 is most suitable and a relatively small concentration of both reactants in equal amounts leads to a self-consistent uniform morphology with smaller size; sufficient ageing time is also required. A tentative formation mechanism involving the fusion, exchange, and coalescence of droplets stuffed with reactants, followed by crystallization of ZnS /surfactant phase with different shapes when the component of system varied, is described. However, the role that surfactant molecules play in nanocrystal formation remains ambiguous, and explicit elucidation based on further experimental work related to the nanostructure of microemulsions is still to be carried out (Xu and Li, 2003)

Zhan *et al.* (2004) study the preparation of nanometer-sized In_2O_3 particles by a reverse microemulsion method. Nanometer-sized indium oxide (In_2O_3) particles have been prepared by chemical reaction of inorganic indium compounds and ammonia gas in a reverse macroemulsion system consisting of water, Triton X-100 (surfactant), n-heptanol (co-surfactant) and n-octane (oil). Precursor hydroxides precipitated in the droplets of water–in–oil (W/O) microemulsion were calcined at different temperatures to form indium oxide powder. The factors affecting the particle size have been discussed; the calcination temperature is considered to be the important factor for controlling the size. In_2O_3 calcined at 400°C had a spherical form and a narrow size distribution. Calcination at 800°C led to the formation of particles not only of irregular shape, but also of a wide size distribution. With the increase in calcinations temperature from 400 to 800 °C, the average size of the particles grew from 7 to about 40 nm. The In_2O_3 nanoparticles were characterized by transmission electron microscopy and X-ray diffraction.

In (2004), the preparation of spherical ultrafine zirconia powder in microemulsion system and its dispersibility were studied by Haung *et al.* (2004) In this work, a water/oil microemulsion consisted of cyclohexane/water/Triton X-100/hexyl alcohol is invented to prepare ultrafine spherical zirconia powder via the reaction which takes place between the precipitant and zirconium salt solved in the nanoreactors. The water droplets in the microemulsion system of cyclohexane /water/Triton X-100/hexyl alcohol can act as the nanoreactors that solubilized zirconium oxychloride and ammonia, respectively. When the above-mentioned two different kinds of the reactors collide, a certain reaction occur and ultrafine spherical zirconia powder with uniform diameter distribution can be obtained in a nanoscale and its diameter is about 30-40 nm. 100% tetragonal crystalline grain of the powder can be obtained when the calcined temperature reaches 500°C. For the powder experienced 800°C calcining temperature, the organic substances on the particle have been nearly burnt out, so it has higher zeta potential than that calcined at temperature 600°C. The powder prepared by microemulsion method has lower content of the soluble contra-ions (Ca^{2+}, Mg^{2+}) than other commercial zirconia powders have.

$600^{\circ}C$. The powder prepared by microemulsion method has lower content of the soluble contra-ions (Ca^{2+}, Mg^{2+}) than other commercial zirconia powders have.

From the development of microemulsion method that used to synthesis the metal oxide, it can conclude that this method has efficiency to prepare the nanoparticle of metal oxide that has high surface area. The condition of microemulsion is the key factor to control the size of reverse micelle (such as structure of surfactant, the ratio of reactant and temperature of the mixing). Because of the tin oxide gas sensor is the important gas sensor. Therefore, this report intends to show the result of the synthesized tin oxide nanoparticles by using microemulsion of the popular nonionic surfactant (Triton X-100) and apply it to the gas sensor application. However, the microemulsion of a new nonionic surfactant (Arlacel P-135), which has different structure compare to the Triton X-100, is also studied and reported.